



# Biofabrication for osteochondral tissue regeneration: bioink printability requirements

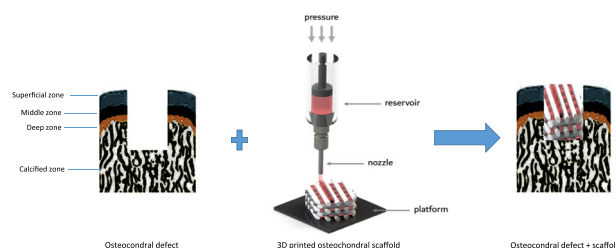
Saba Abdulghani<sup>1</sup> · Pedro G. Morouço<sup>1</sup>

Received: 16 April 2018 / Accepted: 9 January 2019 / Published online: 28 January 2019  
© Springer Science+Business Media, LLC, part of Springer Nature 2019

## Abstract

Biofabrication allows the formation of 3D scaffolds through a precise spatial control. This is of foremost importance when aiming to mimic heterogeneous and anisotropic architecture, such as that of the osteochondral tissue. Osteochondral defects are a supreme challenge for tissue engineering due to the compositional and structural complexity of stratified architecture and contrasting biomechanical properties of the cartilage-bone interface. This review highlights the advancements and retreats witnessed by using developed bioinks for tissue regeneration, taking osteochondral tissue as a challenging example. Methods, materials and requirements for bioprinting were discussed, highlighting the pre and post-processing factors that researchers should consider towards the development of a clinical treatment.

## Graphical Abstract



## 1 Introduction

Osteochondral defects that are most common in the knee [1], may also affect other joints and usually occur in children and young adults [2]. It may be associated with trauma or with other causes of avascular necrosis of bone [3], however, in the majority of cases, no clearly identifiable cause can be found [2]. These defects, affecting both articular cartilage and the underlying subchondral bone are

likely to induce osteoarthritic degenerative changes over time. Aiming to restore biological and mechanical functions to the affected joint, treatment options such as microfracture and autologous osteochondral grafts are utilised [4–7]. However, such procedures have limitations, such as compromised cartilage tissue formation, donor site injury, difficulty in achieving the same shape of the injured site [8]. Engineering the optimum osteochondral construct has proven to be somewhat challenging in the past due to poor tissue formation and problematic integration at the cartilage-bone interface [9].

The osteochondral tissue is a difficult tissue to regenerate naturally owing to its nanostructure of complex stratified architecture and contrasting biomechanical properties [10–12]. In this region, there are four distinct cartilage zones: superficial, middle, deep and calcified. Each zone is defined by a particular composition and organization of cells and extracellular matrix (ECM) molecules, with different proportions of ECM components significantly

✉ Saba Abdulghani  
saba.a.silva@ipleiria.pt

<sup>1</sup> Centre for Rapid and Sustainable Product Development, Polytechnic Institute of Leiria, Rua de Portugal – Zona Industrial, Marinha Grande 2430-028, Portugal

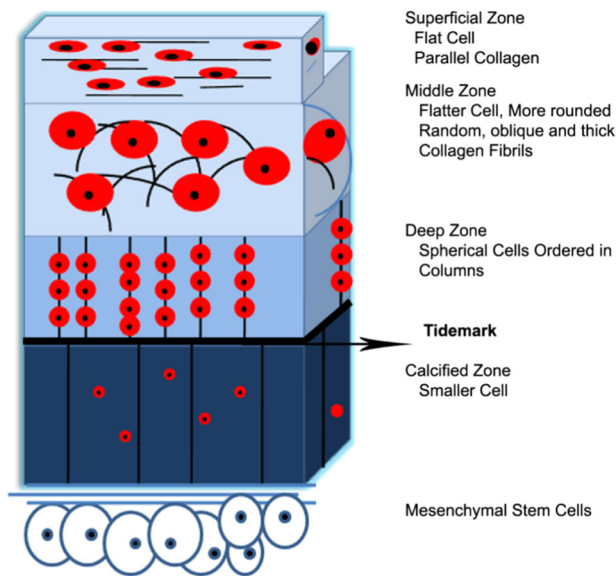


**Fig. 1** Morphology of the articular cartilage. Reproduced from [98], with permission from MDPI

influencing the mechanical properties of each zone [13, 14]. For example, the compressive modulus of superficial, middle and deep zones is 0.079, 2.1 and 320 MPa, respectively, indicating the remarkable differences in stiffness of this tissue (the cartilage zones will be discussed in more details in a following section) [15, 16]. In comparison, subchondral bone is a complex tissue consisting of water, collagen type I and hydroxyapatite crystals, with the two latter components providing the tissue's stiffness and compressive strength respectively [13, 17]. The compressive modulus of subchondral bone is 5.7 GPa, which is higher than that of cartilage, while the tensile modulus is ~2 GPa [16, 18, 19].

The different compositions and mechanical properties of bone and cartilage indicate the complexity of this tissue interface, making it challenging for the design and fabrication of tissue engineering scaffolds [20]. The current tactics have focused on repairing focal cartilage damage, failing in the process to address the entire osteoarthritic joint. The majority of the solutions involve scaffolds that are mechanically inadequate to support the compressive and shear stresses generated in the affected joint. The osteochondral tissue is considered anisotropic in nature, owing to its complicated architecture and properties, therefore any new approach to a new scaffold design should consider this complexity.

To better understand the designing requirements of a scaffold, one must first closely examine the native tissue where the scaffold will be placed. In this case, a comprehensive understanding of the structure and function of the osteochondral tissue will ensure the success of the structure. Hyaline articular cartilage sole function is to provide a

gliding low-friction surface, shock absorption and protecting the underlying subchondral bone from pressure, thus complementing its mechanical strength [11, 21–23]. The compressive properties of the cartilage are based on its proteoglycans. The predominant proteoglycan present in cartilage is the large chondroitin sulphate proteoglycan 'aggrecan'. Following its secretion, aggrecan self-assembles into a supramolecular structure with as many as 50 monomers bound to a filament of hyaluronan. Aggrecan serves a direct, primary role providing the osmotic resistance necessary for cartilage to resist compressive loads [24].

## 2 The properties of the articular cartilage

As mentioned earlier, the compositional and morphological variations in the depth of the cartilage matrix is divided into four distinct zones (Fig. 1) superficial, middle, deep and calcified [11].

- (1) Superficial zone consists of the thinnest densely packed collagen fibres oriented parallel to the articulating surface covering the joint, thus protecting the joint by providing shear resistance and tensile strength. It also monitors fluid permeability and contains cells that secrete lubricants. It takes up to 20% of the total cartilage thickness.
- (2) Middle or transitional zone: is the thickest layer of cartilage, covering 40%–60% of the articular cartilage volume. The collagen fibers in this zone are thick, less organized, and are typically in an oblique to random orientation to the surface. It contains highest proteoglycan content.
- (3) Deep zone: the collagen fibrils are perpendicularly oriented in this zone and delineates at the tidemark thereby differentiating the deep zone from the calcified zone. This arrangement of collagen improves the integration of soft and hard tissues at the cartilage–bone interface. This zone has the highest concentration of proteoglycan and the lowest concentration of water. The collagen fibers traverse the tidemark thus represents a relative change from the deep zone to the zone of calcified cartilage. It covers up to 30% of the total volume of the articular cartilage.
- (4) Calcified zone: is made of collagen X for mineralization and structural integrity. It provides a buffer with intermediate mechanical properties between those of the uncalcified cartilage and the underlying subchondral bone [25, 26].

The deeper zones (middle, deep and calcified zones) have relatively less cell density but thicker collagen bundles (perpendicular to the articulating surface), in comparison to

the superficial zone. They also provide the articulating cartilage with the strength required to resist daily compressive forces. Collectively, these zones contribute to the optimal functioning of the articular cartilage. The maintenance of levels and distribution of proteoglycan and collagen fibres is crucially significant in maintaining the compressive and tensile strengths respectively of the articular cartilage. Biomechanically, the compressive modulus increases from the superficial, zone (0.079 MPa) to the deep zone at 2.10 MPa [13, 14]. On the other hand, the tensile modulus varies in the inverse direction from 25 MPa in the superficial zone to 15 MPa in the deep zone [27, 28].

However, due to the avascular nature of the articular cartilage and the fact that it has a low number of chondrocytes, it has limited regenerative properties [29], which consequently means that most articular cartilage injuries will eventually lead to a more serious condition of osteoarthritis.

In comparison, the subchondral bone's structure is completely different from the cartilage in that it is highly vascularised, thus allowing for its own nourishment as well as the nourishment of the overlaying cartilage [21]. It is composed of concentric lamellar layers around osteons and flat layers representing new bone formation [30]. The peripheral bone is largely avascular, while the endosteal bone is directly adjacent to the calcified cartilage [31]. The subchondral bone serves as an anchorage for the adjacent collagen fibrils and plays an important role in the maintenance of the joint.

### 3 Biofabrication and tissue engineering

Biofabrication is the term used to describe the automated generation of structurally organised and functional biological constructs by combining together living cells, bioactive molecules, biomaterials, cell aggregates such as micro-tissue or hybrid cell-material constructs by means of bioprinting or bioassembly, followed by tissue maturation processes [32–34].

The recent advancements in 3D biofabrication, has permitted the design and fabrication of patient-specific scaffolds that possess structural and functional features comparable to the native tissue. It allows for design and fabrication using tissue images captured with commonly used medical imaging techniques such as computer tomography (CT) and magnetic resonance imaging (MRI) that are readily available in hospitals, something that conventional fabrication techniques lack. The mechanical properties of the developed scaffolds should be directly related to their micro-architectural topology. As such, the permeability of a porous scaffold could be manipulated to mimic the native tissue and to facilitate cell and nutrient movement and allow for a better

host-tissue integration as in osteointegration [35]. Additionally, such structures provide the appropriate micro-environment for cell mechanisms as well as cell-scaffold interaction. Therefore, pore size, porosity, substrate stiffness and orientation are of great importance for the success of the scaffold. Malda et al. compared an organised fibrous scaffold to a random 3D sponge scaffold in cartilage tissue engineering. Their findings demonstrated that chondrogenesis had in fact improved in vivo in the fibrous scaffold due to it being less convoluted in its architecture, thus encouraging diffusion throughout the scaffold [36]. Hedayati et al. [37] investigated the effects of topological design and material type on the mechanical properties of additive manufacturing porous biomaterials. They concluded that a topological design could cause up to 10-fold difference in the mechanical properties of the porous biomaterials while changing the material type had only resulted in up to 2-fold difference. This highlights the importance of scaffold topology on the desired mechanical properties.

As previously mentioned, biofabrication aims to generate constructs through bioassembly or bioprinting. The process of bioassembly refers to the fabrication of hierarchical constructs with prescribed organization by automated assembly [34]. Typically, cell-containing fabrication units are generated via cell-driven self-organization or through preparation of hybrid cell-material building blocks, which can be achieved by enabling technologies, like micro-fabricated moulds or microfluidics [38, 39].

Due to specific challenges imposed by using bioinks (e.g. adequate degradation rate, toxicity of degradation products, immunogenicity) there have been researches focused on engineering tissues composed of only cells and the secreted matrix. This bioassembly strategy aims to fabricate micro-tissues with regular size and shape, which can then be assembled in 3D porous scaffolds [40], enabling the optimization and delivery of individual modules to deliver the necessary tissue-specific organization of cells (Fig. 2).

In contrast, the principle of 3D bioprinting is the layer-by-layer spatial designing and assembling of living cells together with biological cues and biomaterials with a specified organization, forming a 3D living cellular scaffold [33, 41, 42]. It is a highly complicated set-up as the living cells must be delivered in each layer of the scaffold without compromising their viability. It has been demonstrated that using bioprinting methods such as extrusion, inkjet or laser-based printing is not harmful to the viability or the long-term performance of the printed cells [43–45].

Under the extrusion-based 3D printing umbrella are processes such as fused deposition modelling (FDM) and direct ink writing (DIW) that are among the most widely popular methods for 3D scaffold fabrication in the tissue engineering field (Table 1). The principle of extrusion-based printing is that the ink is forced through a nozzle as a

**Fig. 2** Comparison between bottom-up modular assembly approaches and traditional top-down approaches to engineering of complex 3D tissues. Reproduced from [99] with permission from PLOS

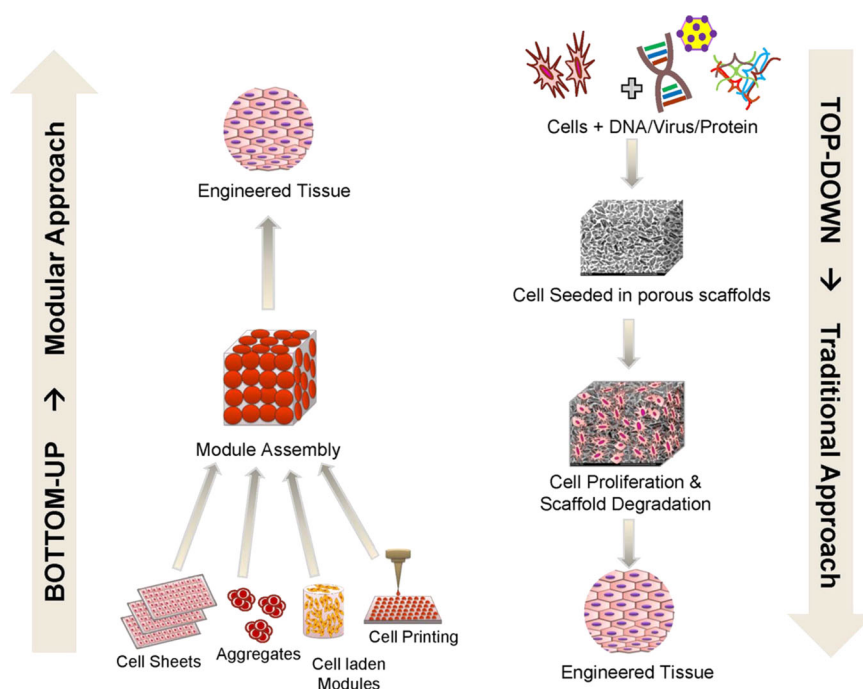


**Table 1** Comparison of the three additive manufacturing approaches for tissue engineering (adapted from [49])

	Jet-based	Extrusion-based	Laser-induced forward transfer
Resolution	+	+/-	++
Fabrication speed	+/-	++	-
Hydrogel viscosity	-	+	+/-
Gelation speed	++	+/-	++
Cell density	-	+	+/-

viscous liquid to form individual lines that solidify upon contact with a substrate (Fig. 3). The technique was introduced in the early 2000s and is the common and affordable bioprinting technique. Accordingly, hydrogels are the most popular ink source in extrusion bioprinting, since they support a load of viable cells, growth factors and/ or genetic material while being extruded from a syringe nozzle.

### 3.1 Natural and synthetic-based bioinks

Bioinks are materials, usually a hydrogel, that mimic an extracellular matrix environment to support the adhesion, proliferation, and differentiation of living cells. Hydrogels are crosslinked 3D polymer networks that are capable of absorbing and retaining large quantities of water. They are divided into two categories: natural (Table 2) and synthetic hydrogels (Table 3).

Natural hydrogels are considered ideal candidate for tissue engineering scaffolds owing to their soft, tissue-like

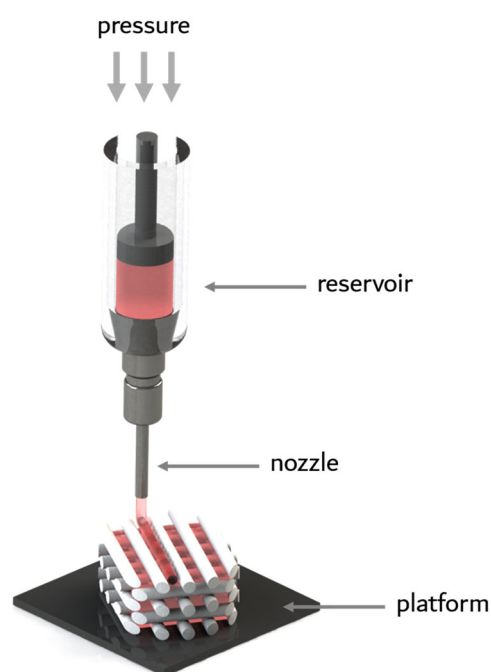


**Fig. 3** Extrusion-based bioprinting setup

properties, which permits cell growth and diffusion of nutrients and waste products. Their advantages over other synthetic scaffolds include the easy control of structural parameters, high water content, biocompatibility and biodegradability, which is considered vital for in vivo applications. Cells can be encapsulated in 3D when the hydrogel undergoes gelation [46, 47]. A disadvantage of hydrogels, is however, their weak mechanical properties and their

inability to maintain their designed shape (rapid degradation) [48], which consequently limit their application in load bearing tissues. Thus, to endure the suitability of a hydrogel for 3D printing, the rheological properties and crosslinking

method (physical or chemical) of the hydrogel must be considered first [49].

### 3.2 Decellularized matrix components

These are bioinks that are based on decellularized extracellular matrix (dECM). The ECM has variable protein compositions, depending on the function it supports. The harvested ECM can be decellularized by extensive washing procedure then used as a bioink [50]. The dECM can be further solubilized into the desired concentration, resulting in a gel-like material suitable for bioprinting. Additionally, the dECM provides a suitable micro-environment for cell proliferation and differentiation as well as a porous structure to maintain bioactive additives into the printed scaffold.

### 3.3 Microcarriers

These are structural components that provide a support system for cell growth and expansion to form multi-cellular aggregates when used in bioprinting. They can be made of synthetic (such as dextran, plastic or glass) or natural (such as cellulose, gelatin or collagen) materials with specified properties [51].

## 4 Scaffold requirements

Several factors must be considered when choosing a material and designing a scaffold for tissue regeneration in general and in particular for osteochondral tissue

**Table 2** Naturally derived hydrogels

Protein-based	Polysaccharide-based	Hybrid natural hydrogels
Collagen	Hyaluronic acid (HA)	Protein/Polysaccharide
Elastin	Agarose	Collagen/HA
Fibrin	Alginate	Lamin/cellulose
Gelatin	Chitosan	Fibrin/alginate
silk		Gelatin/agarose, chitosan, alginate, dextran
Matrigel <sup>TM</sup>		
<b>General advantages</b>		
Inherent biocompatibility		
Biochemical resemblance to the ECM		
Major components of the ECM, provide inherent receptors for cell attachment		
Enzymatic degradation, thus permits scaffold remodelling by cells		
<b>General disadvantages</b>		
Poor mechanical properties, making them unsuitable for load-bearing applications		
Immunogenicity		
Purification		
Limited availability		
Batch-to-batch variability		
Shear thinning		

**Table 3** Synthetically derived hydrogels

Polymer type	Advantages	Disadvantages
Methacrylated gelatin GelMA	High mechanical strength Low swelling ratio Permits mixing with other hydrogels to increase cell survival	low cell proliferation rate Poor bioprinting resolution Poor printing fidelity
Poly(ethylene glycol) PEG	Tailored mechanical properties Hydrophilic » easy diffusion of nutrients and exchange of gases Biocompatible Non-immunogenic PEG derivatives » incorporated into other bioinks as crosslinkers to enhance mechanical properties and printability	Low viscosity in the pure form Lack of cell binding domains
Pluronic acid e.g. Pluronic® F-127	High resolution of the printed construct Forms a gel at room temperature	Only printable at high concentrations of more than 25% w/v Weak mechanical integrity» must be photo-crosslinked Poor cell support and viability



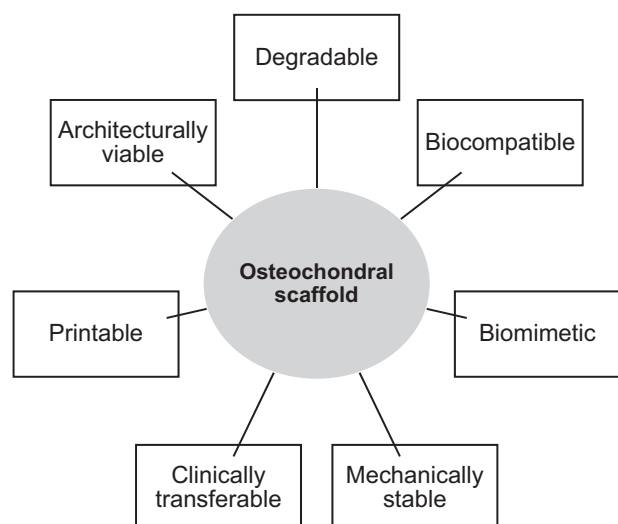


**Fig. 4** Scaffold requirements for osteochondral tissue

regeneration considering the complexity of the osteochondral tissue, Fig. 4.

In general terms, biocompatibility is defined as the ability of a biomaterial to perform its desired function with respect to a medical therapy, without eliciting any undesirable or systemic effects in the recipient or beneficiary of that therapy, but generating the most appropriate beneficial cellular or tissue response in that specific situation, and optimizing the clinically relevant performance of the therapy [52, 53]. In tissue engineering terms, scaffold biocompatibility refers to its ability to support the appropriate cellular activities such as the facilitation of molecular and mechanical signalling systems [54]. The choice of scaffold material plays an important part in influencing the host response at the implant site [53] as biomimicry can be achieved by the incorporation of bioactive features to create an environment that promotes specific cellular response similar to that of the native tissue [55]. In fact, cell behaviour can be influenced simply by incorporating biological stimuli, mechanical forces, and physicochemical material properties [56–58]. For example, hydrogels are able to mimic the native tissue environment as they possess some ECM-like features, allowing them to encapsulate cells in a highly hydrated 3D mechanically stable environment. Moreover, their biocompatibility is influenced by their inherent hydration levels as they possess highly structured polymeric structure, demonstrating up to 40-fold change in volume as they swell or shrink in the presence or absence of water respectively. Additionally, hydrogels can be modified to respond to various physical and biological stimuli [59] such as temperature, light, pH, ions and biochemical signals [60, 61]. They are currently the most widely used scaffold materials in 3D printing due to their easily

controlled functionality, without complex synthesis steps to replicate the native biological tissue's physicochemical properties [60, 62]. Nevertheless, they must meet other certain requirements, in addition to their cell culture suitability, to be considered for bioprinting, such non-immunogenic and have nontoxic byproducts upon degradation. It is also vital that this cytocompatibility is carried on throughout the process of bioprinting, through to in vitro maturation and finally in vivo implantation.

In the case of the osteochondral tissue, and due to its complex structure, a multiple biomimicry approach would be employed in order to reproduce the bone and cartilage phases within a single scaffold such as the use of a biphasic or triphasic scaffold designs. In doing so, subchondral, intermediate and cartilage zonal architecture and function would be taking into consideration, Table 4.

Printability is another vital parameter to be considered when choosing a bioink. It is the ability of the material, once printed layer-by-layer, to form and maintain its structure fidelity and integrity as initially designed. Printability is still an unexplored field that very much requires extensive research. Recently, Ribeiro et al. [63] assessed the shape fidelity of bioinks in an attempt to predict filament collapse directly from the shear stress in a theoretical model. In their study they proposed two quantitative tests based on filament deformation after printing; (i) filament collapse: to assess the deflection and collapse of a suspended filament, (ii) filament fusion which assesses the printed filament's resolution in the x-y plane.




Therefore, based on the above mentioned, two factors are pivotal in determining the fidelity of the printed bioinks:

- (i) Pre-processing factors include the rheological properties of the bioink. These rheological factors include: viscosity, shear thinning, and yield stress,
- (ii) Post-processing: this is mainly to do with the crosslinking mechanisms.

#### 4.1 Pre-processing: rheological properties

In materials science terms, rheology is the study of flow and deformation of materials under applied external stresses/forces. Rheological parameters that play an important role in biofabrication in general and printing fidelity in particular are the viscosity, shear thinning and yield stress. Viscosity is the resistance of a fluid to flow upon application of external force/stress. Hydrogels, as mentioned before, are derived from natural or synthetic polymers and the viscosity of a polymer fluid is dependent on its concentration, molecular weight and temperature. So, in this respect, higher polymer concentration and molecular weight are naturally associated with higher viscosity.

**Table 4** Osteochondral defect scaffolds that reached clinical trial phase (non-3D printed)

Type of scaffold	Biphasic		Triphasic
	Agili-C™ 	TruFi™ 	Maiore-gen™ 
Manufacturer	CartiHeal Ltd, Israel	Smith and Nephew, Andover, MA	Fin-Ceramica, Faenza, Italy
Chemical composition	Bone phase: Calcium carbonate in the form of crystalline aragonite. Cartilage phase: hyaluronic acid	Bone phase: Calcium Sulphate; Cartilage phase: PLGA-PGA (75:25).	Cartilage phase: pure collagen type I; Interface: Collagen type I and HA (60:40); Bone phase: Collagen type I and HA (30:70)

Possessing sufficient viscosity can help bioinks to avoid surface-tension droplet formation and drive it towards continuous strand formation, thus improved shape fidelity and printability. This improvement in printability is due to the fact that the dispensed continuous strands can maintain their cylindrical shape and by doing so they avoid merging with adjacent strands. This is why thermoplastic polymer scaffolds enjoy higher printing accuracy than their hydrogel counterparts. However, in biofabrication, this is a deciding factor for cell-laden scaffolds. A bioink of high viscosity (high polymer concentration) represents a restrictive environment for the cell proliferation, migration and subsequent tissue growth [64], in that the shear stresses associated with high viscosity of the bioink are harmful for the suspended cells [65]. The solution could be the use of low concentrations of high molecular-weight polymers, i.e.

naturally derived hydrogels. Additionally, higher polymer concentrations are usually an indication of superior mechanical properties. Higher polymer densities are more suitable for microextrusion printing since they are more viscous and possess a higher yield stress. It should be noted that higher viscosity inks and higher extrusion forces, coupled with smaller diameter nozzles leads to increased shear forces experienced by the cells during the extrusion process and results in cell death [48, 66]. Shear stresses greater than 60 kPa have been shown to kill greater than 35% of cells during microextrusion [67].

Shear thinning is a term used to describe the non-Newtonian behaviour in polymer fluids, in which the viscosity decreases with increasing shear rate. With increased stress, there is a reorganization of the polymer chains in which they display a more stretched arrangement. Such

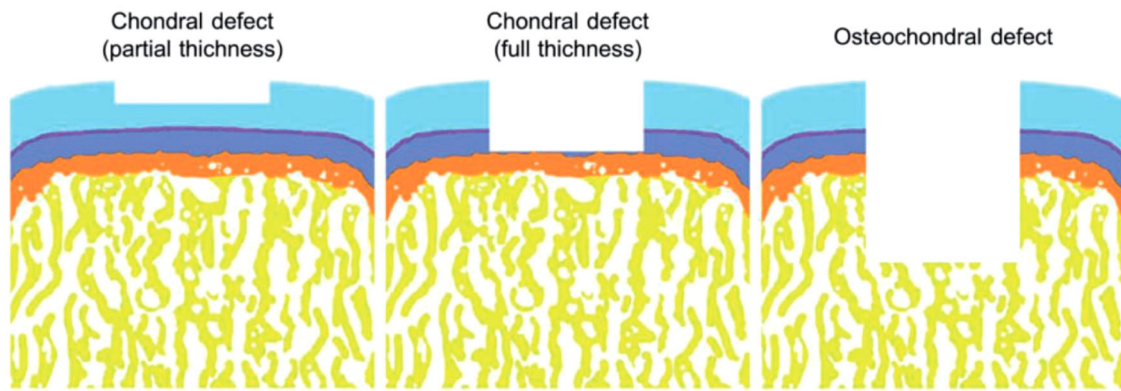


**Fig. 5** Osteochondral defects extending deep into the subchondral bone. Reproduced from [77], with permission from Mary Ann Liebert, Inc

stretching results in less entanglement and consequently a decreased viscosity. For hydrogels, sodium alginate is a good example of a shear thinning behaviour.

In addition to shear thinning, the yield stress also plays an important role in achieving good printability. The yield stress, is the stress needed to be overcome, thus allowing the fluid to flow. It is associated with the deformation of the material. The interactions between the polymer chains generally result in the formation of weak physical crosslinks which are broken by shear forces above the yield stress, however, once these forces are removed, the network reforms again. In the case of high viscosity 3D scaffolds, having a yield stress value can potentially help in preventing flow and collapse, thus improving printability. Additionally, the yield stress helps to prevent cells settling in the hydrogel precursor reservoir. Ribeiro et al. [63] demonstrated recently in a theoretical model the importance of the yield stress in determining the printability of a bioink.

#### 4.2 Post-processing: crosslinking mechanisms

An important parameter for the fidelity of the printed scaffold is the swelling behaviour of the hydrogel. Swelling is a physio-chemical behaviour mainly controlled by the crosslinking mechanism and the charge density. It is considered vital in determining the final shape and size of the printed scaffold [44]. Bencherif [68] showed that densely cross-linked hydrogels, with a high level of methacrylation, are more mechanically robust while maintaining their cytocompatibility and cell adhesion properties.

Physical crosslinking is driven by mechanisms such as ionic, hydrophobic and hydrogen bonding interactions, stereo-complexation and self-assembly of polymers into micellar structures [69]. The ionic type of crosslinking involves the association of polymer chains by non-covalent interactions. A crosslinked hydrogel network is formed when molecules containing opposite charges are blended [70]. Some hydrogels make use of hydrophobic or hydrogen

bonding interactions to crosslink. These kinds of interactions are usually temperature dependant and tend to alter the rheology of the hydrogel. On the other hand, chemical crosslinking of hydrogels involves a covalent bonding between polymer chains and mechanisms such as condensation reactions, Schiff base formation [71] and photocrosslinking [72]. However, it must be noted that there have been some reports of cytotoxicity in chemically crosslinked hydrogels [73].

All the earlier mentioned factors will eventually affect the ‘first layer printability’. To ensure that a printed 3D scaffold maintains its vertical shape, the first printed layer must sustain a large contact angle with the substrate to avoid the destruction of the printed bioink. The first printed layer provides anchorage for the scaffold and ensures its subsequent stability during the entire printing process. A common problem is the use of a glass or plastic slide as a receiving surface for the scaffold, which provides poor contact angle with the printed bioink. To avoid this problem, Campos et al. [74] printed their bioink scaffold in a perfluorotributylamine (C12F27N) hydrophobic high density fluid. Nikkhu et al. [75] coated the printing surface with a thin layer of 3-(trimethoxysilyl) propyl methacrylate to enhance their hydrophobicity and improve printability, while You et al. [76] used polyethylenimine to pre-treat the culture plates, thus ensuring an electrostatic interaction between the printed scaffold and the receiving surface.

### 5 3D-Bioprinting and osteochondral scaffolds

Osteochondral tissue has a complex graded structure where the biology, physiology and mechanics of the region vary drastically along the depth of the tissue making it a very difficult region to treat. Typical osteochondral defects penetrate the entire thickness of the articular cartilage and into the subchondral bone [77] (Fig. 5). Conventional



scaffold fabrication routes such as solvent casting and particle leaching, electrospinning and freeze drying [10, 78, 79] offer limited control over scaffold geometry, pore size and distribution, interconnectivity and internal channel construction and as such there is a decrease in nutrient transport, cell migration and viability particularly in the centre of the scaffold [30]. For example, current osteochondral grafts suffer from poor tissue formation and compromised integration at the interface between the cartilage and the underlying bone layer [9, 80] and between the osteochondral graft and the host tissue [81]. Earlier attempts in osteochondral scaffold fabrication resulted in constructs that were mechanically weak at the interface of cartilage-subchondral bone as they were fabricated in 2 or sometimes 3 parts and glued or sutured together [82, 83].

Biofabrication can offer a huge benefit for the construction of 3D osteochondral scaffolds as it allows for precise mimicking of the native tissue's heterogeneous and anisotropic architecture. This is achieved through a precise special control of bioactive compounds and biomaterials to mimic the biological and mechanical gradient observed in the osteochondral tissue and consequently satisfying the mechanical and compositional requirements of the cartilage and bone tissues. To this end, extensive research has been carried out to develop biphasic or triphasic scaffolds in an effort to mimic the natural gradient of the osteochondral tissue. Holmes et al. [79] developed a PLA biphasic scaffold (with an internal structural feature crossing the length of the scaffold) with collagen surface modification to further enhance the cytocompatibility properties. Their results demonstrated excellent mechanical properties similar or exceeding cartilage (0.75–1 MPa) and subchondral bone (30–50 MPa) in human osteochondral tissue [19, 84]. They also showed that MSC proliferation was greatly enhanced due to the incorporation of the collagen I surface treatment, along with the biomimetically designed micro-features.

Fedorovich et al. [85] used bioplotting to replicate osteochondral tissue by printing two types of osteogenic progenitor cells and chondrocytes into an intricate alginate hydrogel scaffold. Their results, both in vivo and in vitro, revealed distinctive ECM regions formation in different parts of the scaffold. Aiming to improve the mechanical properties of their alginate scaffold, the authors resorted to printing the osteoblast-chondrocyte laden hydrogel in conjunction with a much stronger, mechanically stable poly caprolactone (PCL) as a bone forming scaffold. Their results showed good cellular proliferation after 7 days. Holmes et al designed and 3D printed a series of innovative poly-lactic acid filament with bi-phasic geometry to promote specific stem cell differentiation and improve the mechanical strength and interfacial integration at the osteochondral region of articulate joints. Their bi-phasic scaffolds had enhanced mechanical characteristics in

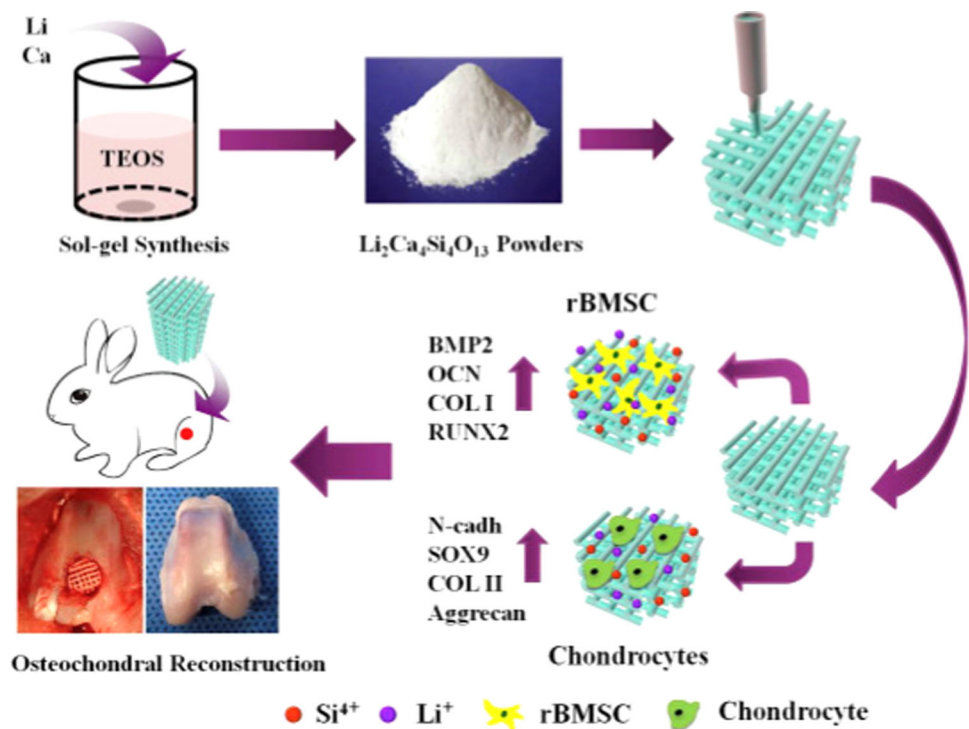
compression (a maximum Young's modulus of 31 MPa) and shear (a maximum fracture strength of 5768 N/mm<sup>2</sup>) when compared with homogenous designs [79].

Nowicki et al. [86] used fused deposition modelling (FDM) 3D bioprinter to produce a complex osteochondral scaffold with a gradient pore distribution and tuneable nHA to improve osteogenic and chondrogenic cell growth. Their results demonstrated improved mechanical and biological performance in an anisotropic pore distribution scaffolds when compared to the homogeneous and non-porous scaffolds [79].

As stated earlier, hydrogels are a favourite choice in 3D bioprinting and although there is a plethora of hydrogels scaffolds for cartilage repair, such as for example 3D printed sodium alginate hydrogel porous construct [87] high-density collagen hydrogel scaffold [88], structurally and functionally optimized silk fibroin/gelatin scaffold [89] these hydrogels, however, seriously lack sufficient mechanical properties and long term mechanical stability in vivo due to the uncontrollable swelling in physiologically aqueous settings. As a result, these hydrogels are unsuitable candidates for load-bearing scaffolds in osteochondral tissue regeneration [90, 91].

Hong and co-workers developed a 3D-printable tough poly(ethylene glycol) (PEG)/sodium alginate hydrogel that displayed a higher fracture toughness (1500 J m<sup>-2</sup>) than that of articular cartilage [92]. More recently, Zhu et al. developed high strength hydrogels as 3D printed bioinks [93] and Yang et al. developed a 3D printed sodium 2-acrylamido-2-methylpropanesulfonate/acrylamide double network hydrogel which exhibited a maximum compression strength of 93.5 MPa [94]. However, these high strength hydrogels and their printability were only made possible through the heavy addition of tackifiers to alter their viscosity. Moreover, UV light irradiation for post-crosslinking with the addition of a photoinitiator was also required in these hydrogels. The addition of the tackifier and initiator may have an adverse effect on the biofunction of the scaffold and/ or impose a potential risk to the patients. Hence, designing and preparing a high strength hydrogel with direct printability and thus printing scaffolds with non-swelling/non-shrinking properties is highly desired. To achieve this, Gao et al. [95] designed a 3D printed biohybrid hydrogel, which demonstrated excellent tensile strength (up to 0.41 MPa), high compressive strength (up to 8.4 MPa) controllable 3D architecture, owing to shear thinning property which allows continuous extrusion through a needle and also immediate gelation of fluid upon deposition on the cooled substrate. In vitro tests showed that by incorporating a transforming growth factor beta 1 (TGF- $\beta$ 1) and  $\beta$ -tricalciumphosphate ( $\beta$ -TCP) on distinct layers within the scaffold to mimic the natural gradient of the osteochondral tissue, has facilitated the attachment, spreading, and chondrogenic and osteogenic

**Fig. 6** 3D printing of a lithium-calcium-silicate crystal bioscaffold with dual bioactivities for osteochondral interface reconstruction. Reproduced from [97] with permission from ScienceDirect



differentiation of human bone marrow stem cells (hBMSCs). Additionally, in vivo experiments in a rat model showed that their 3D-printed biohybrid gradient hydrogel scaffolds significantly and simultaneously increased the regeneration of the cartilage and subchondral bone within the osteochondral defect.

Du et al. [96] produced a multilayer gradient osteochondral scaffold by selective laser sintering (SLS) method that consisted of poly( $\epsilon$ -caprolactone) (PCL) and the hydroxyapatite (HA)/PCL microspheres. The osteochondral zone of the scaffold was made with PCL/HA composite with high HA concentration, whereas the intermediate zone contained a much lower HA concentration and finally the cartilage zone had zero HA concentration. The scaffolds exhibited excellent biocompatibility to support cell adhesion and proliferation in vitro. They also validated their scaffolds in vivo in osteochondral defect using a rabbit model where the acellular scaffolds demonstrated the ability to induce articular cartilage formation by accelerating the early subchondral bone regeneration.

Most recently, Chen et al. [97] investigated the use of high purity bioactive Lithium calcium silicate ( $\text{L}_2\text{Ca}_4\text{S}_4$ ) scaffolds fabricated by 3D-printing to simultaneously regenerate cartilage and subchondral bone, Fig. 6. They successfully prepared highly uniform scaffolds with excellent mechanical strength. Moreover, the in vitro studies demonstrated that at a certain concentration range, the ionic products from their scaffolds significantly stimulated the proliferation and maturation of chondrocytes in addition to

promoting the osteogenic differentiation of rBMSCs. In vivo, they demonstrated that their scaffolds simultaneously promoted the regeneration of both cartilage and subchondral bone as compared to pure  $\beta$ -TCP scaffolds in rabbit osteochondral defects.

At the present time, there are only three gradient scaffolds that are at the clinical trial phase, however, none of them is produced by biofabrication. See Table 4 for scaffold specifications and manufacturer details.

## 6 Conclusions

In this review we discussed the advantages of biofabrication in general and using bioprinting in particular as a tool to precisely mimic the heterogeneous and anisotropic nature of the osteochondral tissue and to closely control the patterning of cells and biological materials which facilitates the production of zonal variations observed in this complex tissue. Some of the used approaches of recent research works have been discussed and it can be concluded that the highly complex native architecture of the osteochondral tissue requires further scaffold development to match its complexity. Future studies should put a significant consideration on the pre-processing aspects, namely the rheological properties, and post-processing factors. A deeper understanding of the mechanical and biological features will surely contribute to important steps toward the translation from labs to clinical settings.

**Acknowledgements** This work was funded by PAMI (ROTEIRO/0328/2013; N° 022158), a Research Infrastructure of the National Roadmap of Research Infrastructures of Strategic Relevance for 2014–2020, co-funded by the FCT and European Union through the Centro2020.

## Compliance with ethical standards

**Conflict of interest** The authors declare that they have no conflict of interest.

**Publisher's note:** Springer Nature remains neutral with regard to jurisdictional claims in published maps and institutional affiliations.

## References

- Easley ME, Cushner FD, Scott WN. Insall & Scott surgery of the knee. Surgery of the Knee. New York, Churchill Livingstone. 2001;1:480.
- Prakash D, Learmonth D. Natural progression of osteo-chondral defect in the femoral condyle. *Knee*. 2002;9:7–10.
- Solomon L, Warwick DJ, Nayagam S. Apley's system of orthopaedics and fractures, Ninth Edition. Malaysian Orthop. 2010;875.
- Marcacci M, Kon E, Delcogliano M, Filardo G, Busacca M, Zaffagnini S. Arthroscopic autologous osteochondral grafting for cartilage defects of the knee: prospective study results at a minimum 7-year follow-up. *Am J Sports Med*. 2007;35(12):2014–21.
- Hangody L, Vászárhelyi G, Hangody LR, Sükösd Z, Tibay G, Bartha L, et al. Autologous osteochondral grafting-technique and long-term results. *Injury*. 2008;39(1 SUPPL.):32–9.
- Kon E, Gobbi A, Filardo G, Delcogliano M, Zaffagnini S, Marcacci M. Arthroscopic second-generation autologous chondrocyte implantation compared with microfracture for chondral lesions of the knee: Prospective nonrandomized study at 5 years. *Am J Sports Med*. 2009;37(1):33–41.
- Lane JG, Healey RM, Chen AC, Sah RL, Amiel D. Can osteochondral grafting be augmented with microfracture in an extended-size lesion of articular cartilage? *Am J Sports Med*. 2010;38(7):1316–23.
- Martin I, Miot S, Barbero A, Jakob M, Wendt D. Osteochondral tissue engineering. *J Biomech*. 2007;40:750–65.
- Schaefer D, Martin I, Shastri P, Padera RF, Langer R, Freed LE, et al. In vitro generation of osteochondral composites. *Biomaterials*. 2000;21(24):2599–606.
- Castro NJ, Hacking SA, Zhang LG. Recent progress in interfacial tissue engineering approaches for osteochondral defects. *Ann Biomed Eng*. 2012;40:1628–40.
- Zhang L, Hu J, Athanasiou KA. The role of tissue engineering in articular cartilage repair and regeneration. *Crit Rev Biomed Eng*. 2009;37(1–2):1–57.
- Zhang L, Webster TJ. Nanotechnology and nanomaterials: promises for improved tissue regeneration. *Nano Today*. 2009;4:66–80.
- Yang PJ, Temenoff JS. Engineering orthopedic tissue interfaces. *Tissue Eng Part B Rev*. 2009;15(2):127–41.
- Keeney M, Pandit A. The osteochondral junction and its repair via bi-phasic tissue engineering scaffolds. *Tissue Eng Part B Rev*. 2009;15(1):55–73.
- Schinagl RM, Gurskis D, Chen AC, Sah RL. Depth-dependent confined compression modulus of full-thickness bovine articular cartilage. *J Orthop Res*. 1997;15(4):499–506.
- Mente PL, Lewis JL. Elastic modulus of calcified cartilage is an order of magnitude less than that of subchondral bone. *J Orthop Res*. 1994;12(5):637–47.
- Arvidson K, Abdallah BM, Applegate LA, Baldini N, Cenni E, Gomez-Barrena E, et al. Bone regeneration and stem cells. *J Cell Mol Med*. 2011;15:718–46.
- Mouser VHM, Levato R, Bonassar LJ, D'Lima DD, Grande DA, Klein TJ, et al. Three-dimensional bioprinting and its potential in the field of articular cartilage regeneration. *Cartilage*. 2017;8:327–40.
- Kelly DJ, Prendergast PJ. Prediction of the optimal mechanical properties for a scaffold used in osteochondral defect repair. *Tissue Eng*. 2006;12(9):2509–19.
- Stoop R. Smart biomaterials for tissue engineering of cartilage. *Injury*. 2008;39(1 SUPPL.):77–87.
- Nukavarapu SP, Doremus DL. Osteochondral tissue engineering: current strategies and challenges. *Biotechnol Adv*. 2013;31:706–21.
- Bhosale AM, Richardson JB. Articular cartilage: structure, injuries and review of management. *Br Med Bull*. 2008;87:77–95.
- Toh WS, Spector M, Lee EH, Cao T. Biomaterial-mediated delivery of microenvironmental cues for repair and regeneration of articular cartilage. *Mol Pharm*. 2011;8:994–1001.
- Aspberg A. Cartilage proteoglycans. In: *Cartilage: Volume 1: physiology and development*. 2016. p. 1–22.
- Poole AR, Kojima T, Yasuda T, Mwale F, Kobayashi M, Lavery S. Composition and structure of articular cartilage: a template for tissue repair. *Clin Orthop Relat Res*. 2001;1(391 Suppl):S26–33.
- Goldring MB, Marcu KB. Cartilage homeostasis in health and rheumatic diseases. *Arthritis Res Ther*. 2009;11(3):224.
- Holland TA, Tabata Y, Mikos AG. Dual growth factor delivery from degradable oligo(poly(ethylene glycol) fumarate) hydrogel scaffolds for cartilage tissue engineering. *J Control Release*. 2005;101:111–25.
- Harley BA, Lynn AK, Wissner-Gross Z, Bonfield W, Yannas IV, Gibson LJ. Design of a multiphase osteochondral scaffold III: fabrication of layered scaffolds with continuous interfaces. *J Biomed Mater Res - Part A*. 2010;92(3):1078–93.
- Almaraz AJ, Athanasiou KA. Design characteristics for the tissue engineering of cartilaginous tissues. *Ann Biomed Eng*. 2004;32(1):2–17.
- Ozolat IT. Bioprinting of osteochondral tissues: A perspective on current gaps and future trends. *Int J Bioprinting*. 2017;3(2):1–12.
- Clark JM, Huber JD. The structure of the human subchondral plate. *J Bone Jt Surg Br*. 1990;72:866–73.
- Moroni L, Burdick JA, Highley C, Lee SJ, Morimoto Y, Takeuchi S, et al. Biofabrication strategies for 3D in vitro models and regenerative medicine. *Nature Reviews Materials*. 2018;3:21–37.
- Groll J, Boland T, Blunk T, Burdick JA, Cho DW, Dalton PD, et al. Biofabrication: reappraising the definition of an evolving field. *Biofabrication*. 2016;8:013001.
- Moroni L, Boland T, Burdick JA, De Maria C, Derby B, Forgacs G, et al. Biofabrication: a guide to technology and terminology. *Trends Biotechnol*. 2018;36(4):384–402.
- Liu X, Wu S, Yeung KWK, Chan YL, Hu T, Xu Z, et al. Relationship between osseointegration and superelastic biomechanics in porous NiTi scaffolds. *Biomaterials*. 2011;32(2):330–8.
- Malda J, Woodfield TBF, Van Der Vloodt F, Wilson C, Martens DE, Tramper J, et al. The effect of PEGT/PBT scaffold architecture on the composition of tissue engineered cartilage. *Biomaterials*. 2005;26(1):63–72.
- Hedayati R, Ahmadi SM, Lietaert K, Pouran B, Li Y, Weinans H, et al. Isolated and modulated effects of topology and material type on the mechanical properties of additively manufactured porous biomaterials. *J Mech Behav Biomed Mater*. 2018;79:254–63.

38. Fu CY, Tseng SY, Yang SM, Hsu L, Liu CH, Chang HY. A microfluidic chip with a U-shaped microstructure array for multicellular spheroid formation, culturing and analysis. *Biofabrication*. 2014;6(1):5009.
39. Young C, Rozario K, Serra C, Poole-Warren L, Martens P. Poly (vinyl alcohol)-heparin biosynthetic microspheres produced by microfluidics and ultraviolet photopolymerisation. *Biomicrofluidics*. 2013;7(4):44109.
40. Schon BS, Hooper GJ, Woodfield TBF. Modular tissue assembly strategies for biofabrication of engineered cartilage. *Ann Biomed Eng*. 2017;45:100–14.
41. Murphy SV, Atala A. 3D bioprinting of tissues and organs. *Nat Biotechnol*. 2014;32:773–85.
42. Ozbolat IT, Hospodiuk M. Current advances and future perspectives in extrusion-based bioprinting. *Biomaterials*. 2016;76:321–43.
43. Visser J, Peters B, Burger TJ, Boomstra J, Dhert WJA, Melchels FPW, et al. Biofabrication of multi-material anatomically shaped tissue constructs. *Biofabrication*. 2013;5(3):5007.
44. Schuurman W, Levett PA, Pot MW, van Weeren PR, Dhert WJA, Hutmacher DW, et al. Gelatin-methacrylamide hydrogels as potential biomaterials for fabrication of tissue-engineered cartilage constructs. *Macromol Biosci*. 2013;13(5):551–61.
45. Cui X, Breitenkamp K, Lotz M, D'Lima D. Synergistic action of fibroblast growth factor-2 and transforming growth factor-beta1 enhances bioprinted human neocartilage formation. *Biotechnol Bioeng*. 2012;109(9):2357–68.
46. Kim JE, Kim SH, Jung Y. Current status of three-dimensional printing inks for soft tissue regeneration. *Tissue Eng Regen Med*. 2016;13:636–46.
47. Tan H, Marra KG. Injectable, biodegradable hydrogels for tissue engineering applications. *Mater (Basel)*. 2010;3(3):1746–67.
48. Billiet T, Vandenhaute M, Schelfhout J, Van Vlierberghe S, Dubrue P. A review of trends and limitations in hydrogel-rapid prototyping for tissue engineering. *Biomaterials*. 2012;33:6020–41.
49. Malda J, Visser J, Melchels FP, Jüngst T, Hennink WE, Dhert WJA, et al. 25th anniversary article: Engineering hydrogels for biofabrication. *Adv Mater*. 2013;25:5011–28.
50. Ott HC, Matthiesen TS, Goh SK, Black LD, Kren SM, Netoff TI, et al. Perfusion-decellularized matrix: Using nature's platform to engineer a bioartificial heart. *Nat Med*. 2008;14(2):213–21.
51. Malda J, Frondoza CG. Microcarriers in the engineering of cartilage and bone. *Trends Biotechnol*. 2006;24:299–304.
52. Greenwald AS. Biological performance of materials. *Fundamentals of Biocompatibility*. J Bone Jt Surg. 2001;83(6):970.
53. Williams DF. On the mechanisms of biocompatibility. *Biomaterials*. 2008;29(20):2941–53.
54. Gaharwar AK, Sant S, Hancock MJ, Hacking SA. Nanomaterials in tissue engineering: fabrication and applications. *Nanomaterials in Tissue Engineering: Fabrication and Applications*. 2013.
55. Vyas C, Poologundarampillai G, Hoyland J, Bartolo P. 3D printing of biocomposites for osteochondral tissue engineering. In: *Biomedical Composites (Second Edition)*. Woodhead Publishing Series in Biomaterials. 2017, p. 261–302.
56. Stevens MM, George JH. Exploring and engineering the cell surface interface. *Science*. 2005;310(5751):1135–8.
57. Place ES, Evans ND, Stevens MM. Complexity in biomaterials for tissue engineering. *Nat Mater*. 2009;8(6):457–70.
58. Crowder SW, Leonardo V, Whittaker T, Papathanasiou P, Stevens MM. Material cues as potent regulators of epigenetics and stem cell function. *Cell Stem Cell*. 2016;18(1):39–52.
59. Morouço P, Lattanzi W, Alves N. Four-dimensional bioprinting as a new era for tissue engineering and regenerative medicine. *Front Bioeng Biotechnol*. 2017;5:61.
60. Gaharwar AK, Peppas NA, Khademhosseini A. Nanocomposite hydrogels for biomedical applications. *Biotechnol Bioeng*. 2014;111(3):441–53.
61. Xu K, Wang J, Chen Q, Yue Y, Zhang W, Wang P. Spontaneous volume transition of polyampholyte nanocomposite hydrogels based on pure electrostatic interaction. *J Colloid Interface Sci*. 2008;321(2):272–8.
62. Utech S, Boccaccini AR. A review of hydrogel-based composites for biomedical applications: enhancement of hydrogel properties by addition of rigid inorganic fillers. *J Mater Sci*. 2016;51:271–310.
63. Ribeiro A, Blokzijl MM, Levato R, Visser CW, Castilho M, Hennink WE, et al. Assessing bioink shape fidelity to aid material development in 3D bioprinting. *Biofabrication*. 2017;10(1):4102.
64. Nicodemus GD, Bryant SJ. Cell encapsulation in biodegradable hydrogels for tissue engineering applications. *Tissue Eng Part B Rev*. 2008;14(2):149–65.
65. Aguado BA, Mulyasmita W, Su J, Lampe KJ, Heilshorn SC. Improving viability of stem cells during syringe needle flow through the design of hydrogel cell carriers. *Tissue Eng Part A*. 2012;18(7–8):806–15.
66. Blaeser A, Duarte Campos DF, Puster U, Richtering W, Stevens MM, Fischer H. Controlling shear stress in 3D bioprinting is a key factor to balance printing resolution and stem cell integrity. *Adv Healthc Mater*. 2016;5(3):326–33.
67. Nair K, Gandhi M, Khalil S, Yan KC, Marcolongo M, Barbee K, et al. Characterization of cell viability during bioprinting processes. *Biotechnol J*. 2009;4(8):1168–77.
68. Bencherif SA, Srinivasan A, Horkay F, Hollinger JO, Matyjaszewski K, Washburn NR. Influence of the degree of methacrylation on hyaluronic acid hydrogels properties. *Biomaterials*. 2008;29(12):1739–49.
69. Jungst T, Smolan W, Schacht K, Scheibel T, Groll J. Strategies and molecular design criteria for 3D printable hydrogels. *Chem Rev*. 2016;116:1496–539.
70. Gulrez SK, Al-Assaf S, Phillips GO. Hydrogels: Methods of preparation, characterisation and applications in molecular and environmental bioengineering. *Prog Mol Environ Bioeng - From Anal Modelling to Technol Appl*. 2011;646.
71. Dragan ES. Design and applications of interpenetrating polymer network hydrogels. A review. *Chem Eng J*. 2014;243:572–90.
72. Wang Z, Abdulla R, Parker B, Samanipour R, Ghosh S, Kim K. A simple and high-resolution stereolithography-based 3D bioprinting system using visible light crosslinkable bioinks. *Biofabrication*. 2015;7(4):045009.
73. Hennink WE, van Nostrum CF. Novel crosslinking methods to design hydrogels. *Adv Drug Deliv Rev*. 2012;64:223–36.
74. Duarte Campos DF, Blaeser A, Weber M, Jäkel J, Neuss S, Jähnen-Dechent W, et al. Three-dimensional printing of stem cell-laden hydrogels submerged in a hydrophobic high-density fluid. *Biofabrication*. 2013;5(1):5003–13.
75. Nikkha M, Eshak N, Zorlutuna P, Annabi N, Castello M, Kim K, et al. Directed endothelial cell morphogenesis in micropatterned gelatin methacrylate hydrogels. *Biomaterials*. 2012;33(35):9009–18.
76. You F, Wu X, Zhu N, Lei M, Eames BF, Chen X. 3D Printing of porous cell-laden hydrogel constructs for potential applications in cartilage tissue engineering. *ACS Biomater Sci Eng*. 2016;2(7):1200–10.
77. Li X, Ding J, Wang J, Zhuang X, Chen X. Biomimetic biphasic scaffolds for osteochondral defect repair. *Regen Biomater*. 2015;2(3):221–8.
78. Wang M, Cheng X, Zhu W, Holmes B, Keidar M, Zhang LG. Design of biomimetic and bioactive cold plasma-modified nanostructured scaffolds for enhanced osteogenic differentiation



- of bone marrow-derived mesenchymal stem cells. *Tissue Eng Part A*. 2014;20(5–6):1060–71.
79. Holmes B, Zhu W, Li J, Lee JD, Zhang LG. Development of novel three-dimensional printed scaffolds for osteochondral regeneration. *Tissue Eng Part A*. 2015;21(1–2):403–15.
  80. Gao J, Dennis JE, Solchaga LA, Awadallah AS, Goldberg VM, Caplan AI. Tissue-engineered fabrication of an osteochondral composite graft using rat bone marrow-derived mesenchymal stem cells. *Tissue Eng*. 2001;7(4):363–71.
  81. Theodoropoulos JS, De Croos JNA, Park SS, Pilliar R, Kandel RA. Integration of tissue-engineered cartilage with host cartilage: An in vitro model. *Clin Orthop Relat Res*. 2011;469:2785–95.
  82. Rodrigues MT, Lee SJ, Gomes ME, Reis RL, Atala A, Yoo JJ. Bilayered constructs aimed at osteochondral strategies: the influence of medium supplements in the osteogenic and chondrogenic differentiation of amniotic fluid-derived stem cells. *Acta Biomater*. 2012;8(7):2795–806.
  83. Miot S, Brehm W, Dickinson S, Sims T, Wixmerten A, Longinotti C, et al. Influence of in vitro maturation of engineered cartilage on the outcome of osteochondral repair in a goat model. *Eur Cells Mater*. 2012;23:222–36.
  84. Newitt DC, Majumdar S, Van Rietbergen B, Von Ingersleben G, Harris ST, Genant HK, et al. In vivo assessment of architecture and micro-finite element analysis derived indices of mechanical properties of trabecular bone in the radius. *Osteoporos Int*. 2002;13(1):6–17.
  85. Fedorovich NE, Schuurman W, Wijnberg HM, Prins HJ, van Weeren PR, Malda J, et al. Biofabrication of osteochondral tissue equivalents by printing topologically defined, cell-laden hydrogel scaffolds. *Tissue Eng Part C Methods*. 2012;18(1):33–44.
  86. Nowicki MA, Castro NJ, Plesniak MW, Zhang LG. 3D printing of novel osteochondral scaffolds with graded microstructure. *Nanotechnology* 2016;27(41):4001–10.
  87. Markstedt K, Mantas A, Tournier I, Martínez Ávila H, Hägg D, Gatenholm P. 3D bioprinting human chondrocytes with nanocellulose-alginate bioink for cartilage tissue engineering applications. *Biomacromolecules*. 2015;16(5):1489–96.
  88. Rhee S, Puetzer JL, Mason BN, Reinhart-King CA, Bonassar LJ. 3D Bioprinting of spatially heterogeneous collagen constructs for cartilage tissue engineering. *ACS Biomater Sci Eng*. 2016;2(10):1800–5.
  89. Das S, Pati F, Choi YJ, Rijal G, Shim JH, Kim SW, et al. Bio-printable, cell-laden silk fibroin-gelatin hydrogel supporting multilineage differentiation of stem cells for fabrication of three-dimensional tissue constructs. *Acta Biomater*. 2015;11(1):233–46.
  90. Chung JHY, Naficy S, Yue Z, Kapsa R, Quigley A, Moulton SE, et al. Bio-ink properties and printability for extrusion printing living cells. *Biomater Sci*. 2013;1(7):763.
  91. Ouyang L, Highley CB, Rodell CB, Sun W, Burdick JA. 3D Printing of shear-thinning hyaluronic acid hydrogels with secondary cross-linking. *ACS Biomater Sci Eng*. 2016;2(10):1743–51.
  92. Hong S, Sycks D, Chan HFA, Lin S, Lopez GP, Guilak F, et al. 3D Printing: 3D printing of highly stretchable and tough hydrogels into complex, cellularized structures. *Adv Mater*. 2015;27(27):4034.
  93. Zhu F, Cheng L, Wang ZJ, Hong W, Wu ZL, Yin J, et al. 3D-Printed ultratough hydrogel structures with titin-like domains. *ACS Appl Mater Interfaces*. 2017;9(13):11363–7.
  94. Yang F, Tadepalli V, Wiley BJ. 3D Printing of a double network hydrogel with a compression strength and elastic modulus greater than those of cartilage. *ACS Biomater Sci Eng*. 2017;3(5):863–9.
  95. Gao F, Xu Z, Liang Q, Liu B, Li H, Wu Y, et al. Direct 3D printing of high strength biohybrid gradient hydrogel scaffolds for efficient repair of osteochondral defect. *Adv Funct Mater*. 2018;28:1706644–56.
  96. Du Y, Liu H, Yang Q, Wang S, Wang J, Ma J, et al. Selective laser sintering scaffold with hierarchical architecture and gradient composition for osteochondral repair in rabbits. *Biomaterials*. 2017;137:37–48.
  97. 3D printing of a lithium-calcium-silicate crystal bioscaffold with dual bioactivities for osteochondral interface reconstruction. *Biomaterials*. 2018.
  98. Doulabi AH, Mequanint K, Mohammadi H. Blends and nanocomposite biomaterials for articular cartilage tissue engineering. *Mater (Basel)*. 2014;7(7):5327–55.
  99. Tiruvannamalai-Annamalai R, Armant DR, Matthew HWT. A glycosaminoglycan based, modular tissue scaffold system for rapid assembly of perfusable, high cell density, engineered tissues. *PLoS One*. 2014;9(1):e84287.